Uniosun Journal of Engineering and Environmental Sciences (UJEES), Vol. 8 No. 2, Sept., 2026
DOI: 10.64980/ujees.v8i2.025 **Julius et al.**
Published: September 30, 2026

NUMERICAL STUDY OF SURFACE SUCTION EFFECTS ON THE AERODYNAMIC PERFORMANCE OF A NACA 4412 AIRFOIL AT LOW REYNOLDS NUMBERS

Moses O. JULIUS[1*], Saheed A. ADIO[2], Ayowumi R. SOJI-ADEKUNLE[3], Fatai. A. BUHARI[4], Tolulope E. AREMU[5]

[1]*Department of Aerospace Engineering, Obafemi Awolowo University, Ile-Ife, Osun State, Nigeria*

[2]*Department of Mechanical Engineering, Obafemi Awolowo University, Ile-Ife, Osun State, Nigeria*

[3]*Department of Mechanical Engineering, Adeleke University, Ede, Osun State, Nigeria*

[4]*Department of Agricultural and Biosystem Engineering, Adeleke University, Ede, Osun State, Nigeria*

[5]*Department of Agricultural and Biosystem Engineering, Adeleke University, Ede, Osun State, Nigeria*

[*]*Corresponding Author: mojulius@oauife.edu.ng*

Abstract

Early separation of the boundary layer and the appearance of a Laminar Separation Bubble (LSB) can result in reduced lift and increased drag at low Reynolds numbers. The aerodynamic performance of a National Advisory Committee for Aeronautics (NACA) 4412 airfoil is numerically studied in the present work, under the influence of suction at its surface, with two-dimensional Computational Fluid Dynamics (CFD) simulations in ANSYS Fluent. The influence of suction on lift coefficient, drag coefficient, pressure coefficient distribution and LSB characteristics was assessed by simulations performed at Reynolds numbers of 25,000, 35,000, 45,000 and 50,000 for various angles of attack. The Transition SST turbulence model was used to properly simulate the transition behaviour and separation phenomena. Suction was applied through a 0.002 w/c slot located on the upper surface over $0.20 < x/c < 0.40$, with suction coefficients (C_q) of 0.002, 0.003 and 0.005. The results show that the aerodynamics of the airfoil can be significantly enhanced by the use of surface suction, which can energise the boundary layer and inhibit flow separation. At 25,000 Re and an angle of attack of 10°, the lift coefficient increased from 0.833 to 1.020 (22.5%), while the drag coefficient decreased from 0.200 to 0.170 (15.0%). Using pressure coefficient analysis, at 50,000 Re and angle of attack of 8°, it was found that the suction peak at the leading edge was increased by 9–15% and the pressure plateau at the LSB was completely removed. At a suction coefficient (C_q) of 0.002, the length of the LSB was decreased to 0.10c (66.7%), but the suction coefficients of 0.003 and 0.005 fully eliminated the LSB. Overall, surface suction progressively suppressed the laminar separation bubble, reducing its length by 66.7% at 0.002 C_q and completely eliminating it at 0.003 C_q and 0.005 C_q, which corresponded to improved aerodynamic performance through increased lift and reduced drag.

Keywords
NACA 4412, Boundary Layer Suction, Transition SST, Laminar Separation Bubble, Suction Control Technique.

1. INTRODUCTION

The performance of the airfoil is always considered in the design and operation of aerospace vehicles in low-speed aerodynamics [1]. In recent decades, unmanned aerial vehicles (UAVs), micro aerial vehicles (MAVs), small-scale reconnaissance aircraft and small-scale wind energy systems have been taking the centre of research interests, leading to enhanced interest in aerodynamic behaviour under low Reynolds number [2]. As opposed to conventional aircraft where flights are mostly performed in the high Reynolds number regime, the range of Reynolds numbers for such systems often traverses a host of complex viscous flow phenomena, flow sensitivity and unstable boundary layer behaviour [3]. At low Reynolds numbers, however, the aerodynamic performance is important for the production of lift, drag and manoeuvrability, flight endurance and flight stability.

For low Reynolds number aerodynamics, the study of flow behaviour is always dominated by viscous phenomena and transitions [4], [5]. In this flow regime, the boundary layer is mostly laminar over the full

chord of the airfoil, and is very vulnerable to adverse pressure gradients and early onset of flow separation [6]. One of the most important flow phenomena occurring during low Reynolds number operation, when separation of the laminar boundary layer results in the subsequent transition of the separated shear layer to turbulent boundary layer with a downstream reattachment is known as the laminar separation bubble (LSB) [7]. The pressure distribution over the airfoil surface changes drastically for separation, which can lead to reattachment under specific conditions, but adds further aerodynamic penalties with the presence of the separation bubble. This flow instability can lead to an increase in the drag coefficient, decrease in lift generation, fluctuating aerodynamic forces and stall onset early in the flight [8]. Also, the laminar separation bubble may be of different size, location and nature, which are highly sensitive to Reynolds number, angle of attack, airfoil shape and surface conditions, making low Reynolds number aerodynamics very hard to predict accurately [9]. On the other hand, the adverse pressure effects that occur in low Reynolds number flows become more pronounced in the case of a decrease in Reynolds number. In such instances, the separated shear layer may not reattach, resulting in massive flow separation and a loss of aerodynamic efficiency [10]. This is especially a problem for small-scale aerodynamic systems, where the typical operating Reynolds number is less than 10^5. In addition to its impact on the lift-to-drag ratio, low Reynolds number flow instability can result in unsteady aerodynamic loading and reduced controllability and/or performance inconsistency during flight conditions [11].

Among the numerous airfoil geometries investigated in aerodynamic research, the NACA 4412 airfoil has been found to possess many desirable aerodynamic characteristics, and it has been used in many different engineering applications. The NACA 4412 is a four-digit cambered airfoil with a maximum camber of 4.0% at 40.0% of the chord length, and a thickness ratio of 12% relative to chord length. It has a moderate camber setting which allows for the generation of relatively high lift, but with acceptable drag characteristics over the operating range [12]. However, at lower Reynolds numbers, the NACA 4412 becomes increasingly dominated by transitional flow phenomena and effects of laminar separation. Also, variations in lift coefficient, drag coefficient and stall characteristics have been demonstrated by previous investigations to occur on the airfoil depending on Reynolds number and angle of attack [13]. Laminar separation bubbles in the vicinity of the leading edge or the mid-chord are especially significant in terms of altering the surface pressure distribution, which leads to a rise in drag and decrease in aerodynamic efficiency. Several studies have also reported that for sufficiently low Reynolds number values, the airfoil experiences boundary layer separation very early, resulting in a reduction in lift performance and unstable aerodynamic characteristics [14], [15].

Hence, active flow control methods have become of great interest due to their potential to achieve enhanced aerodynamic efficiency under adverse flow conditions. Active flow control is similar to passive flow control strategies, but requires the introduction of external energy or momentum to the flowfield, which alters the behaviour of the boundary layer to delay flow separation [16]. There are various active control techniques for low Reynolds number applications, with the most promising being surface suction. In surface suction, fluid particles in the boundary layer with low momentum are removed by a suction slot or porous surface, and the momentum of the near-wall flow is increased, thereby enhancing the capability of the boundary layer to withstand adverse pressure gradients [16], [17] . The mechanism can either delay or prevent separation, reduce the separation bubble size and enhance the pressure recovery on the surface of the airfoils [18]. The previous investigations have shown that if the suction is applied properly, a significantly better lift coefficient can be achieved with a reduction in drag coefficient, as well as the postponement of stall onset and the improvement in lift-to-drag ratio [16], [19], [20]. A few of these suction control studies have also revealed that, in many instances, it altered the pressure distributions and resulted in increased flow attachment on the suction side. Many factors, however, such as location of suction, intensity of suction, slot geometry and operating Reynolds number, greatly influence the suction ability. Also, the effect of suction in the region close to the leading edge has been reported to result in better separation suppression than other methods [21].

The flow control by suction on cambered airfoils, like the NACA 4412, has been studied by several researchers. Studies reported that the use of suction control provides advantages to enhance the aerodynamic efficiency of the flow under low Reynolds number conditions, [12], [18]. Other studies reported an appreciable drag decrease and postponement of separation with suction near the separation region close to the leading edge, while others reported increases in the pressure recovery and suppression of the laminar separation bubble on the suction surface [22], [23]. Even with these favourable results, there are a lot of inconsistencies concerning the optimal suction parameter required for maximum aerodynamic improvement. Furthermore, many previous studies were conducted under fixed Reynolds number or limited operating conditions, making it difficult to draw a general conclusion about the suction efficiency under different low Reynolds number conditions. Therefore, the present work aims to study the effect of surface suction on the aerodynamic behaviour of a NACA 4412 airfoil under various low Reynolds numbers, especially with a view to determine optimal slot width and suction strength, quantify the suction effect on aerodynamic loads at different Reynolds numbers and quantify LSB suppression.

2. NUMERICAL METHOD

The NACA coordinate equations were used to develop the airfoil geometry. All the geometric parameters inside the computational domain were then scaled to the airfoil chord length. The C-type computational domain for the airfoil was made large enough to prevent the boundary conditions from having an appreciable effect on the aerodynamic solution. This was done with a 15c upstream boundary and a 25c downstream boundary. The upper and lower limits were 20c away from the airfoil surface. Computational Fluid Dynamics (CFD) was employed for analysis of the aerodynamic behaviour of a NACA 4412 airfoil at low Reynolds numbers. The investigation was based on the steady-state, two-dimensional, and incompressible flow assumptions and was focused on the development of the lift and drag characteristics and pressure distribution for the formation of the laminar separation bubble (LSB). Numerical simulations were carried out based on the Reynolds-averaged Navier-Stokes (RANS) equations, as presented in Equation 1 and Equation 2, solved numerically by the finite-volume method, with the software ANSYS Fluent [16].

The continuity equation is given as:

$$\frac{\partial u_i}{\partial x_i} = 0 \tag{1}$$

where u_i denotes the velocity component in the i_{th} coordinate direction and x_i represents the spatial coordinate.

The momentum equation is:

$$\rho u_j \frac{\partial u_i}{\partial x_j} = -\frac{\partial p}{\partial x_i} + \mu \frac{\partial^2 u_i}{\partial x_j^2} - \rho \frac{\partial \overline{u_i u_{j'}}}{\partial x_j} \tag{2}$$

ρ is fluid density, p is the static pressure, μ is dynamic viscosity, u_i and u_j are velocity components and $\overline{u_i u_{j'}}$ is the Reynolds stress arising from turbulence fluctuations.

In the governing equations, the Reynolds stress tensor introduces additional unknowns, which requires closure through an appropriate turbulence model. However, this study employed a Transition SST model. The model features an intermittency and transition momentum-thickness Reynolds number transport equation that is added to the Shear Stress Transport (SST) model as presented in Equations 3 to 7. This enables the simulation to capture the progression from laminar to turbulent flow and maintain robustness under adverse pressure gradient conditions [24], [25].

The SST $k-\omega$ Transport equation for turbulent kinetic energy is given by:

$$\frac{\partial(\rho k)}{\partial t} + \frac{\partial(\rho u_j k)}{\partial x_j} = P_k - \beta^* \rho k\omega + \frac{\partial}{\partial x_j}\left[(\mu + \sigma_k \mu_t)\frac{\partial k}{\partial x_j}\right] \tag{3}$$

The SST $k-\omega$ Transport equation for specific dissipation rate is written as:

$$\frac{\partial(\rho\omega)}{\partial t} + \frac{\partial(\rho u_j \omega)}{\partial x_j} = \alpha \frac{\omega}{k} P_k - \beta \rho \omega^2 + \frac{\partial}{\partial x_j}\left[(\mu + \sigma_\omega \mu_t)\frac{\partial \omega}{\partial x_j}\right] + 2(1-F_1)\rho\sigma_{\omega 2}\frac{1}{\omega}\frac{\partial k}{\partial x_j}\frac{\partial \omega}{\partial x_j} \tag{4}$$

The Intermittency transport equation is given by:

$$\frac{\partial(\rho\gamma)}{\partial t} + \frac{\partial(\rho u_j \gamma)}{\partial x_j} = P_\gamma - E_\gamma + \frac{\partial}{\partial x_j}\left[\left(\mu + \frac{\mu_t}{\sigma_f}\right)\frac{\partial \gamma}{\partial x_j}\right] \tag{5}$$

The Transition momentum thickness Reynolds number equation is:

$$\frac{\partial(\rho Re_{\theta t})}{\partial t} + \frac{\partial(\rho u_j Re_{\theta t})}{\partial x_j} = P_{\theta t} + \frac{\partial}{\partial x_j}\left[\sigma_{\theta t}(\mu + \mu_t)\frac{\partial Re_{\theta t}}{\partial x_j}\right] \tag{6}$$

The SST model computes turbulent viscosity as

$$\mu_t = \frac{\rho k}{max\left(\omega, \frac{SF_2}{a_1}\right)} \tag{7}$$

where k is turbulent kinetic energy, P_k production of turbulent kinetic energy, ω is the specific dissipation rate, μ is the molecular viscosity, μ_t is the turbulent viscosity, α, $\sigma_{\omega 2}$, a, a_1, β^* are model constants. F_1 is the SST blending function that combines the $k-\omega$ is the model constant.

The governing equations were discretised by the finite volume method (FVM) in ANSYS Fluent. The SIMPLE algorithm was employed in order to obtain a pressure – velocity coupling, and second-order spatial discretisation schemes were used for all the transport equations to reduce the numerical diffusion. Turbulent intensity and turbulent viscosity ratio of 0.3% and 1, respectively, were used at the inlet boundary. Solution convergence was judged based on monitoring of the continuity, momentum, turbulence and transition equation residuals and was considered converged when the residuals in all four equations were reduced to 10^{-5}. Furthermore, the lift and drag coefficients were checked as well to ensure numerical convergence and physical convergence. Six increasingly fine C-type meshes were used, and the same computational domains, boundary conditions and solver parameters were employed in a grid independence study as presented in Table 1. The aim of the first-layer height is to meet the requirement near the wall, which is y+<1 on the Transition SST model. The increase in lift coefficient and decrease in drag coefficient increased with mesh

refinement, though the difference between meshes was less significant as more refinement was added. The lift change is relative to the previous mesh, and the difference in lift coefficient between Meshes M4 and M6 was less than 0.2%, and the difference in drag coefficient was negligible. For this reason, it was decided to use Mesh M4 (near 2.64 × 10^5 cells) for all of the simulations, as it yielded the right balance between computational accuracy and efficiency. The suction coefficient was estimated using the expression in Equation 8. In order to validate the present numerical data, the coefficient of lift was compared with the experimental values of Genc et al. (2016). Genc et al. (2016) worked on the characteristics of the NACA 4412 aerofoil at low Reynolds number. The present work shows good agreement with the experimental data sets as shown in Figure 1. The slight variations between the present data and the experimental data could be a result of some uncertainties, such as the type of turbulence model used.

$$C_q = \frac{V_s}{U_\infty} \tag{8}$$

Table 1: Mesh Independent Study

Mesh	Cells	Nodes	First Layer Height (m)	Average (y^+)	C_L	C_D	Change in (C_L) (%)
M1 (Coarse)	82,450	43,120	1.8×10^{-5}	0.92	0.691	0.1898	—
M2	128,760	66,540	1.5×10^{-5}	0.89	0.701	0.1869	1.45
M3	184,530	94,310	1.2×10^{-5}	0.84	0.706	0.1852	0.71
M4	263,940	134,870	1.0×10^{-5}	0.81	0.708	0.1846	0.28
M5	356,780	181,560	8.5×10^{-6}	0.79	0.709	0.1842	0.14
M6 (Finest)	492,610	249,830	7.0×10^{-6}	0.76	0.7095	0.1840	0.07

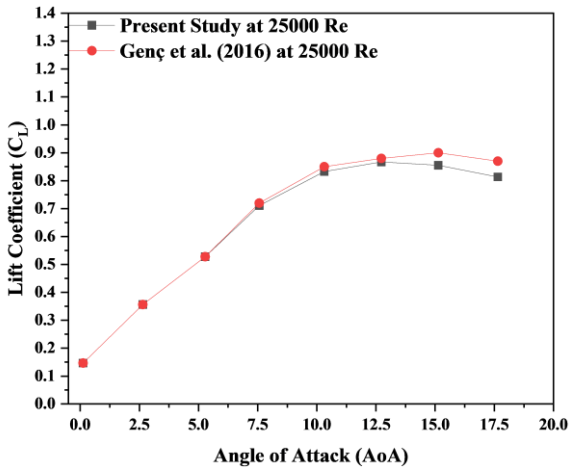


Fig. 1: Comparison between lift coefficient of present numerical work and experimental results

3. RESULTS AND DISCUSSION

The results and discussion focus on the effects of suction location and strength on the lift and drag coefficients, pressure coefficient distribution, and laminar separation bubble characteristics to elucidate the underlying flow-control mechanisms.

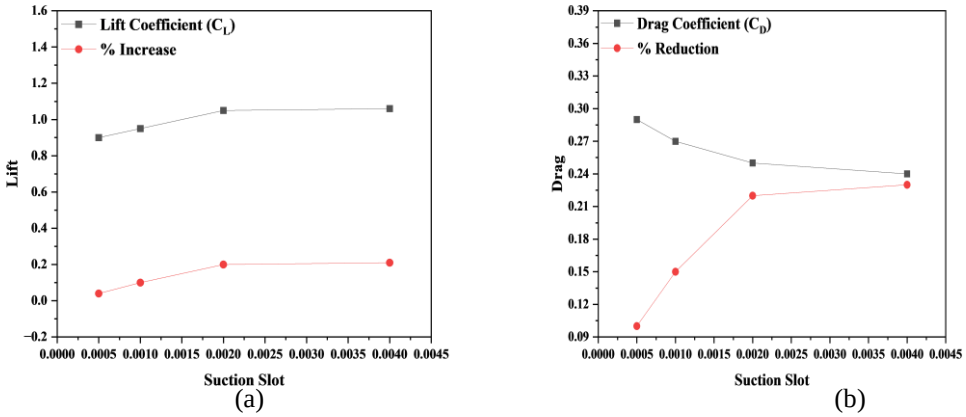
3.1 Effect of Suction Slot Width on Aerodynamic Performance at 25,000 Re and 8° AoA

The influence of suction slot width on the aerodynamic performance of the NACA 4412 airfoil was investigated at a Reynolds number of 25,000, 0.003 C_q and an angle of attack of 8°, as shown in Table 2. As shown in Figure 2, increasing the non-dimensional slot width from 0.0005 w/c to 0.004 w/c resulted in a progressive improvement in aerodynamic performance. The lift coefficient increased from 0.90 to 1.06, while the drag coefficient in Figure 2a decreased from 0.29 to 0.24, corresponding to an overall lift enhancement and drag reduction of approximately 17.8% and 17.2%, respectively. The observed improvements are attributed to the increased slot widths, which enhance boundary-layer momentum by continuously removing low-energy fluid from the near-wall region. At the low Reynolds number considered, the laminar boundary layer is highly susceptible to adverse pressure gradients and early flow separation. Stronger suction delays boundary-layer separation, promotes flow attachment over a greater portion of the airfoil surface, and improves pressure recovery, thereby increasing lift while simultaneously reducing pressure drag. A notable increase in lift was observed as the slot width increased from 0.0005 w/c to 0.002 w/c, whereas only marginal improvement occurred between 0.002 w/c and 0.004 w/c. Similarly, the reduction in drag became less

pronounced at the largest slot width, indicating diminishing aerodynamic returns with increasing suction strength. The results indicate that a moderate suction slot width (w/c equals 0.002) provides an effective compromise between aerodynamic improvement and suction requirement, making it a practical configuration for low-Reynolds-number airfoil applications, which was selected for the research.

Table 2: Slot Width

Case	Slot Width (mm)	Non-dimensional (w/c)
A	0.5	0.0005
B	1	0.001
C	2	0.002
D	4	0.004



(a) (b)

Fig. 2: Effect of Suction Slot on (a) Lift Coefficient (b) Drag Coefficient

3.2 Effect of Suction Strength on Laminar Separation Bubble Characteristics at 25,000 Re and of 8° AoA

The effects of suction strength (C_q) on the characteristics of the Laminar Separation Bubble (LSB) of the NACA 4412 airfoil at 25,000 Re and an angle of attack of 8° are summarised in Figure 3. In the baseline case (C_q equals 0), flow separation occurred at 0.20 x/c and reattached at 0.50 x/c, producing an LSB length of 0.30c. This relatively large separation bubble is an indication of a high level of boundary-layer instability, which negatively impacts pressure recovery and aerodynamic performance. The boundary layer behaviour changed with progressive introduction of surface suction, which led to a delay in the onset of separation and an earlier reattachment. At 0.001 C_q, the separation point shifted downstream to 0.22 x/c, while the reattachment point moved upstream to 0.45 x/c, reducing the bubble length by 23.3% to 0.23c. As the suction strength increased to 0.002 C_q, separation was further delayed to 0.25 x/c while reattachment was advanced to 0.35 x/c, corresponding to a large reduction in LSB (66.7% of baseline). When the suction strength was further increased to 0.003 C_q, no separation or reattachment points were identified, and the laminar separation bubble disappeared. This same behaviour was retained at 0.005 C_q, where the boundary layer remained attached all over the surface of the airfoil under the applied suction. As suction is increased, this total suppression of LSB is seen to be a confirmation that the increased suction strength energises the low-momentum layer and thus aids in overcoming the adverse pressure gradient without separation.

3.3 Effect of Surface Suction on Lift Coefficient

The lift coefficient (C_L) is shown in Figure 4 as a function of angle of attack for the NACA 4412 airfoil with and without surface suction at Reynolds numbers of 25,000, 35,000, 45,000 and 50,000. Overall, surface suction always improved the lift coefficient at all angles of attack, but more or less for different Reynolds numbers and flow conditions. When suction strength of 0.003 was applied, the lift increase was small at low angles of attack because the baseline flow was mostly attached. For example, at 25,000 Re in Figure 4d, the lift coefficient increased from 0.147 to 0.165 at approximately 0°, representing a 12.5% improvement. This effect of suction became more dominant as the angle of attack increased because of the increasing adverse pressure gradient. At 10°, the lift coefficient increased by 22.5%, 20.2%, 18.6%, and 21.4% for Reynolds numbers of 25,000, 35,000, 45,000, and 50,000, respectively. The increased lift is thought to be caused by the capacity of suction to energise the boundary layer, to delay flow separation, and to maintain the low-pressure area above the upper boundary surface. High suction values were seen in the near-stall region, where the greatest benefit of suction was observed. In the baseline cases, the maximum lift coefficient was obtained and then dropped off quickly due to large-scale flow separation. At 50,000 Re in Figure 4a, for instance, the baseline lift dropped from 1.25 at 16.2° to 0.82 at 17.3°, indicating the onset of stall. The suction-controlled airfoil, by contrast, showed effective stall suppression, maintaining a lift coefficient of 1.32 at the same angle. Suction was seen to have similar effects to the other Reynolds numbers, causing flow separation to be

delayed and maintaining lift past the baseline stall angle. The results show that the surface suction is a very effective way of enhancing lift generation, as it ensures the attachment of the boundary layers, prevents the formation of laminar separation bubbles and delays the stall. This improvement is especially noticeable at moderate to high AoAs, where flow separation is the most significant aspect of the aerodynamic response of the airfoil under low Reynolds number flow regimes.

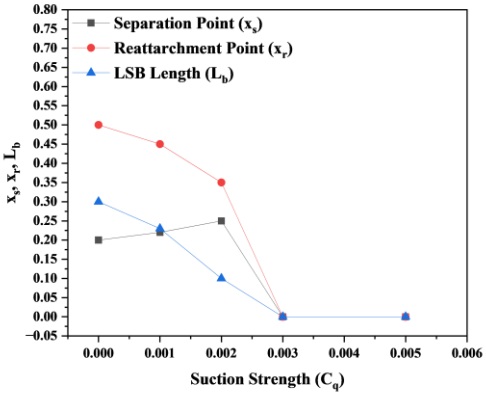


Fig. 3: Laminar Separation Characteristics

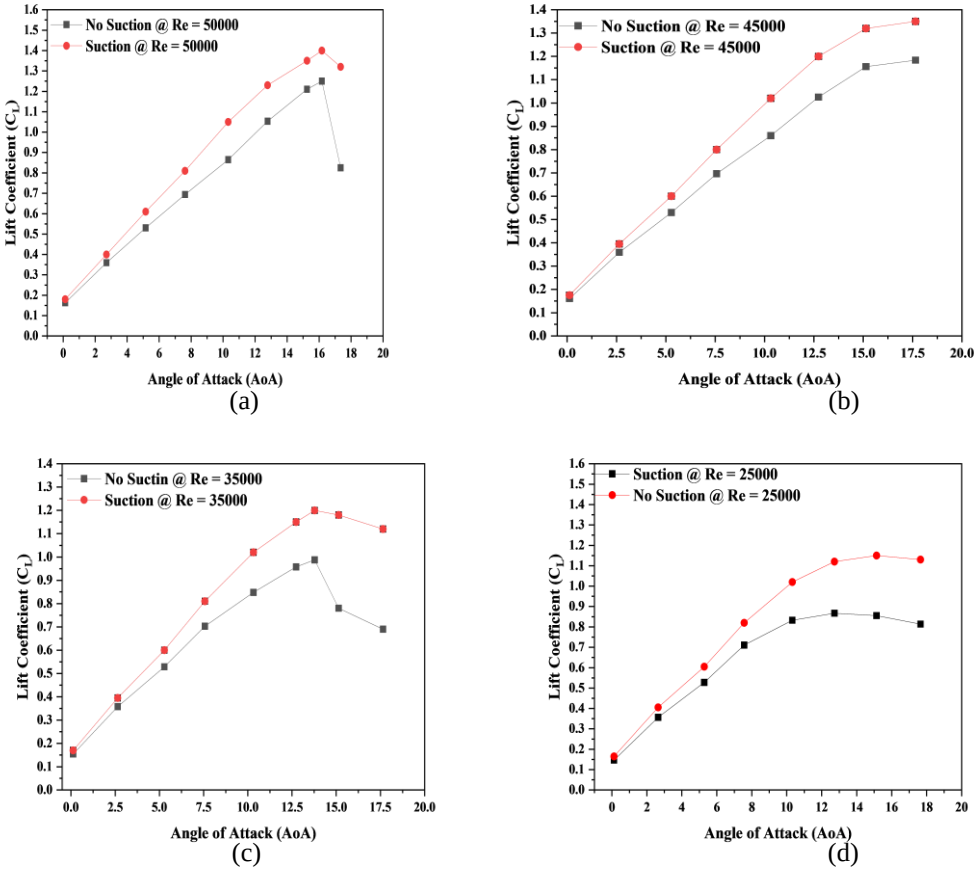
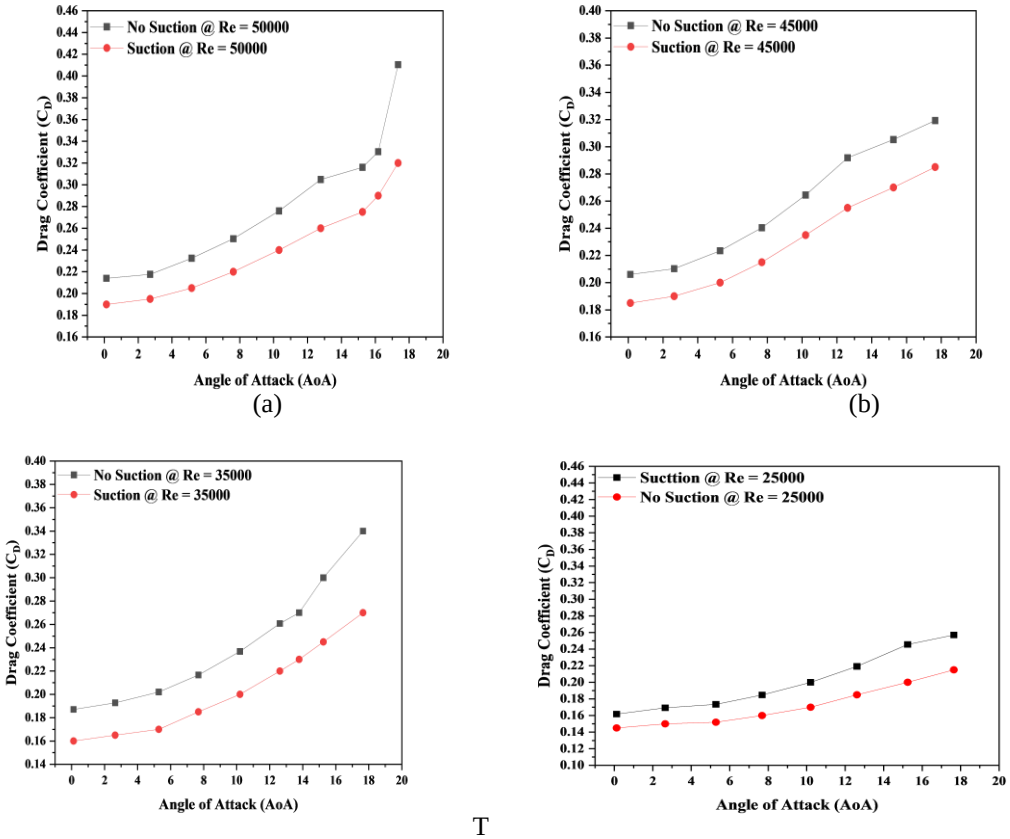


Fig. 4: Effect of 0.003 C_q on Lift Coefficient at (a) 50000 Re (b) 45000 Re (c) 35000 Re (d)25000 Re

3.4 Effect of Surface Suction on Drag Coefficient

Figure 5 shows the drag coefficient (C_D) against angle of attack for the NACA 4412 airfoil (with and without surface suction) at the following Reynolds numbers: 25,000, 35,000, 45,000 and 50,000. The drag coefficient was lowered by this surface suction of 0.003 C_q at all angles of attack, and was lowered more at moderate and high angles where flow separation was more apparent. The drag reduction at low angles of attack was not significant as the boundary layer was still mostly attached in the baseline configuration. For example, at approximately 0° in Figure 5d, the drag coefficient decreased from 0.162 to 0.145 at 25,000 Re, representing a 10.3% reduction, while reductions of 14.5%, 10.2%, and 11.2% were obtained at Reynolds numbers of 35,000, 45,000, and 50,000, respectively. The effectiveness of the suction increased with the increase in the

angle of attack. At approximately 10°, the drag coefficient was reduced by 15.0% (25,000 Re), 15.5% (35,000 Re), 11.1% (45,000 Re), and 13.0% (50,000 Re), indicating that suction effectively mitigated separation-induced pressure drag. The greatest improvement was in the stall region, with the baseline airfoil showing a significant increase in drag with large boundary-layer separation. At 50,000 Re in Figure 5a, the drag coefficient increased sharply from 0.330 at 16.2° to 0.410 at 17.3°, whereas the suction-controlled case increased more gradually from 0.290 to 0.320, corresponding to a 22.0% reduction in drag at the highest angle of attack. The same behaviour was seen at all other Reynolds numbers, as well as suction delaying flow separation and limiting separated wake growth. The drag reduction is believed to be due to the surface suction's ability to remove low-momentum fluid from the boundary layer, keeping the flow attached, enhancing pressure recovery, and decreasing the pressure drag.



T

Fig. 5: Effect of 0.003 C_q on Drag Coefficient at (a) 50000 Re (b) 45000 Re (c) 35000 Re (d)25000 Re

3.5 Effect of Surface Suction on Pressure Coefficient Distribution

The pressure coefficient (C_p) distributions of the NACA 4412 airfoil with and without surface suction are compared at Re of 25,000, 35,000, 45,000 and 50,000 for an angle of attack of 8° and suction strength of 0.003 as presented in Figure 6. Surface suction consistently yielded increased negative pressure coefficient on the upper (suction) surface, especially in the leading-edge region (0.02 x/c to 0.30 x/c), which translates to greater flow acceleration and aerodynamic loading. The peak suction at x/c equals 0.02 increased from −1.35 to −1.55 (14.8%) at 25,000 Re in Figure 6a, from −1.45 to −1.60 (10.3%) at 35,000 Re in Figure 6b, from −1.55 to −1.70 (9.7%) at 45,000 Re in Figure 6c, and from −1.60 to −1.75 (9.4%) at 50,000 Re in Figure 6d. These results show that the leading-edge suction peak is enhanced by the suction, derived from the maintenance of an attached high-momentum boundary layer. For 25,000 Re, a distinct pressure plateau appears in the baseline pressure distributions within the range 0.20 x/c to 0.50 x/c, and it gets progressively smaller as Re increases. A nearly constant pressure region is one of the characteristics of a laminar separation bubble (LSB), which has a separated shear layer with very little pressure recovery before reattachment. At all Reynolds numbers, the pressure coefficient on the lower surface decreases smoothly. As expected, the LSB plateau is eliminated, indicating that suction has an effect on decreasing the boundary-layer separation and the occurrence of a laminar separation bubble. In both the baseline and the suction cases, pressure distribution on the lower (pressure) surface remained essentially unchanged, suggesting that the aerodynamic improvements are primarily due to changes in the upper surface boundary layer. Therefore, the greater lift coefficient and lower value of drag coefficient are accounted for by the increased pressure difference between the upper and lower surfaces. The progressive increase in the suction peak, and the eventual disappearance of the LSB plateau, illustrate the significant improvement in the pressure recovery and flow

attachment to the surface, in other words, the aerodynamic efficiency, over the entire Reynolds number range studied.

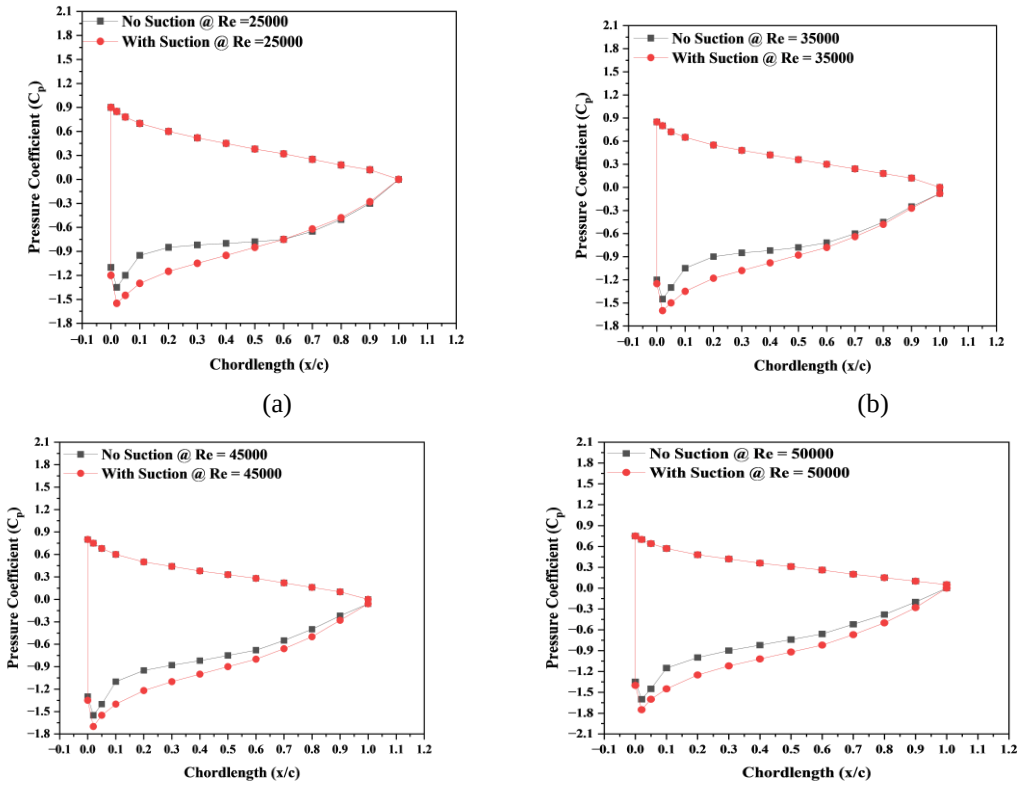


Fig. 5: Effect of 0.003 C_q on Pressure Coefficient at 8° AoA for (a) 50000 Re (b) 45000 Re (c) 35000 Re (d)25000 Re

3.6 Effect of Reynolds Number on Laminar Separation Bubble under Surface Suction

Figure 7 shows the effect of Reynolds number on the laminar separation bubble (LSB) for the baseline and suction-controlled cases at an angle of attack of 8°. Without suction, the LSB length decreased progressively with increasing Reynolds number, from 0.30c at 25,000 Re to 0.07c at 50,000 Re. The decrease is due to the thicker boundary layer momentum at high Reynolds numbers that allows the flow to better resist the adverse pressure gradient, delay separation, and encourage early reattachment. As a result, the separation bubble is reduced in length, thus achieving better natural aerodynamic performance. The laminar separation bubble was completely removed for all Reynolds numbers involved by applying surface suction. In the suction cases, no separation or reattachment locations were observed, and the boundary layer was attached over the airfoil surface. This behaviour illustrates how this low-momentum fluid is removed from the near-wall region by the effective use of suction, thus preventing the formation of a laminar separation bubble. The separation bubble was found to be the largest for the baseline case (0.30c) at 25,000 Re. This is because the complete suppression of LSB under suction has led to significant improvements in lift and a reduction in drag at this Reynolds number. Suction was found to keep the flow attached even with the natural decrease in the baseline LSB as the Reynolds number increased, and it was found to reduce separation losses and improve pressure recovery as the Reynolds number increased.

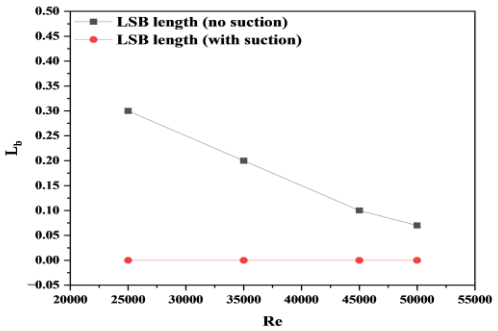


Fig. 6: LSB length

4. CONCLUSION

Two-dimensional CFD simulations of the aerodynamic performance of a NACA 4412 airfoil were performed in the ANSYS Fluent software to explore the influence of surface suction on the aerodynamic performance at Reynolds numbers in the range of 25000 to 50000. Results show that surface suction has a significant positive influence on the aerodynamics by stabilising the boundary layer, postponing flow separation and inhibiting the formation of laminar separation bubbles (LSBs). The lift coefficient was always enhanced, and the drag coefficient was always decreased with all Reynolds numbers examined. The lift coefficient rose by 22.5%, from 0.833 to 1.020, while the drag coefficient fell by 15.0%, from 0.200 to 0.170, at 25,000 Re and 10° AoA. These enhancements were also found at higher Reynolds numbers, and the percentage increase in lift ranges from 18.6% to 22.5%, while the percentage decrease in drag varies from 11.1% to 15.5%. The post-stall loss was also delayed with the application of suction, keeping the lift coefficient at 1.32 at 17.3° and 50,000 Re, compared to the sharp post-stall drop in lift coefficient to 0.82 for the baseline airfoil. Pressure coefficient analysis showed that the suction enhanced the leading-edge suction peak by ~9-15%, removed the typical LSB pressure plateau, and enhanced the pressure recovery over the suction surface. Moreover, the LSB length reduced from 0.30c to 0.10c (i.e., a 66.7% decrease) as the suction coefficient was increased from 0 to 0.002, and it was eliminated at a suction coefficient of 0.003 and 0.005. The Reynolds number range was used to observe that suction would prevent the separation of the baseline LSB throughout the range studied, regardless of the baseline LSB size. All in all, the results showed that properly applied surface suction is a good active flow-control measure for enhancing the aerodynamic efficiency of the NACA 4412 airfoil at low Reynolds numbers.

However, the results of the study must be considered with regard to its limitations. Two-dimensional steady Reynolds-averaged Navier–Stokes (RANS) simulations and the Transition SST turbulence model were used for the analysis and 3D flow structures and unsteady separation dynamics were not completely captured. The results were not confirmed in experiment and the suction power needed to create power was not measured. Moreover, the investigation was limited to Reynolds numbers ranging from 25,000 to 50,000 and an optimum suction location was not determined, nor was a net energy benefit. Energy benefit should be added to future work, together with three dimensional unsteady RANS (URANS) and if possible large eddy simulation (LES). Future research is also needed to systematically optimise suction location and operating strength and quantify the power consumption of the suction systems to calculate the net aerodynamic and energy benefits of Active Flow Control (AFC).

REFERENCES

[1] Pangas, G. F. S., and Gamboa, P. V. (2025). Low-speed airfoil optimization for improved off-design performance. *Aerospace, 12*(8), 685. https://doi.org/10.3390/aerospace12080685

[2] Candeloro, P., Ragni, D., and Pagliaroli, T. (2022). Small-scale rotor aeroacoustics for drone propulsion: A review of noise sources and control strategies. *Fluids, 7*(8), 279. https://doi.org/10.3390/fluids7080279

[3] Chen, L., Guo, Z., Deng, X., and Hou, Z. (2020). Aerodynamic performance and transition prediction of low-speed fixed-wing unmanned aerial vehicles in full configuration based on improved γ–Re model. *Aerospace Science and Technology, 107*, 106281. https://doi.org/10.1016/j.ast.2020.106281

[4] Giacomini, E., and Westerberg, L.-G. (2025). CFD analysis of transition models for low-Reynolds number aerodynamics. *Applied Sciences, 15*(18), 10299. https://doi.org/10.3390/app151810299

[5] Julius, M., Adio, S., Adekunle, A. S., Ishaq, A., Fatai, B., and Akingbade, T. (2025). Unsteady aerodynamic performance of spiked and unspiked Aloe Vera-inspired aerofoils at low Reynolds number. *LAUTECH Journal of Engineering and Technology, 19*(1), 54–64. https://doi.org/10.36108/laujet/5202.91.0150

[6] Toppings, C., and Yarusevych, S. (2025). Low-Reynolds-number aerofoil boundary layer transition in large-scale free stream turbulence. *Journal of Fluid Mechanics, 1021*, A46. https://doi.org/10.1017/jfm.2025.10747

[7] Mo, J., and Rho, B. (2020). Characteristics and effects of laminar separation bubbles on NREL S809 airfoil using the γ–Reθ transition model. *Applied Sciences, 10*(17), 6095. https://doi.org/10.3390/app10176095

[8] Eljack, E. M. (2024). The structure and dynamics of the laminar separation bubble. *Journal of Fluid Mechanics, 998*, A56. https://doi.org/10.1017/jfm.2024.855

[9] Brunelli, C., Avirovic, M., Janssens, B., Marinus, B. G., Hillewaert, K., and Runacres, M. (2026). Prediction of laminar separation bubble on airfoils at low Reynolds number. *Flow, Turbulence and Combustion, 116*(2), 27. https://doi.org/10.1007/s10494-025-00727-7

[10] Cimarelli, A., Corsini, R., and Stalio, E. (2024). Reynolds number effects in separating and reattaching flows with passive scalar transport. *Journal of Fluid Mechanics, 984*, A20. https://doi.org/10.1017/jfm.2024.215

[11] Martínez-Muriel, C., Viola, I. M., García-Villalba, M., and Flores, O. (2025). Mitigating unsteady loads at low Reynolds numbers using a passive trailing-edge flap. *Journal of Fluids and Structures, 138*, 104392. https://doi.org/10.1016/j.jfluidstructs.2025.104392

[12] Li, J. (2025). Aerodynamic characteristics of NACA2412 and NACA4412 at low Reynolds number numerical simulation. *Applied and Computational Engineering, 156*(1), 186–195. https://doi.org/10.54254/2755-2721/2025.MH25948

[13] Rayhan, A. M., Hossain, M. S., Mim, R. H., and Ali, M. (2024). Computational and experimental study on the aerodynamic performance of NACA 4412 airfoil with slot and groove. *Heliyon, 10*(11), e31595. https://doi.org/10.1016/j.heliyon.2024.e31595

[14] Julius, M. O., Ishaq, A. A., Buhari, F. A., Opeyemi, T., and Timileyin, T. (2024). Bio-inspired aerofoils: Unsteady flow analysis of Aloe Vera wing profile with spike at low Reynolds numbers. *Adeleke University Journal of Engineering and Technology, 7*(2), 137–147.

[15] Thompson, E. B., and Gunasekaran, M. (2021). Review analysis on laminar separation bubble at low Reynolds numbers. *Journal of Physics: Conference Series, 2054*(1), 012005. https://doi.org/10.1088/1742-6596/2054/1/012005

[16] Julius, M. O., Adio, S. A., Muritala, A. O., and Alonge, O. (2020). The suction control characteristics of flow separation on NACA 23012. *East African Journal of Engineering, 2*(1), 1–15. https://doi.org/10.37284/eaje.2.1.121

[17] Wang, A., and Lai, H. (2024). Control of separated flow at low Reynolds number around NACA0012 airfoil by boundary layer suction. *Journal of Physics: Conference Series, 2707*(1), 012122. https://doi.org/10.1088/1742-6596/2707/1/012122

[18] Atzori, M., Vinuesa, R., Fahland, G., Stroh, A., Gatti, D., Frohnapfel, B., and Schlatter, P. (2020). Aerodynamic effects of uniform blowing and suction on a NACA4412 airfoil. *Flow, Turbulence and Combustion, 105*(3), 735–759. https://doi.org/10.1007/s10494-020-00135-z

[19] Aloukili, A. M., Elsakka, M., Ali, M., and Elrefaei, M. (2024). Numerical investigation of the suction and blowing effects on the performance of S826 aerofoil for wind turbine applications. *Journal of Al-Azhar University Engineering Sector, 19*(72), 117–130. https://doi.org/10.21608/auej.2024.253920.1510

[20] Elsayed, A. M., Khalifa, M. A., Benini, E., and Aziz, M. A. (2023). Experimental and numerical investigations of aerodynamic characteristics for wind turbine airfoil using multi-suction jets. *Energy, 275*, 127503. https://doi.org/10.1016/j.energy.2023.127503

[21] Yousefi, K., and Saleh, R. (2015). Three-dimensional suction flow control and suction jet length optimization of NACA 0012 wing. *Meccanica, 50*(6), 1481–1494. https://doi.org/10.1007/s11012-015-0100-9

[22] Balaji, K., and Wessley, G. J. (2021). Enhancement of aerodynamic efficiency of aerofoil using improved blowing and suction system. *Advances in Science and Technology Research Journal, 15*(2), 116–126. https://doi.org/10.12913/22998624/134642

[23] Grappadelli, M. C., Olivucci, P., and Badrya, C. (2023). Effects of boundary layer suction on a laminar separation bubble on a HLFC wing. In *AIAA AVIATION 2023 Forum*. American Institute of Aeronautics and Astronautics. https://doi.org/10.2514/6.2023-3955

[24] Julius, M. O., Ishaq, A. A., Buhari, F. A., Opeyemi, T., and Taiwo, T. (2024). Unsteady aerodynamic performance of Aloe Vera-inspired aerofoil without spike at low Reynolds numbers. *Adeleke University Journal of Engineering and Technology, 7*(2), 148–157.

[25] Song, H., Ma, M., Yi, C., Shao, Z., Bai, R., and Yan, C. (2024). An innovative modification to the Menter shear-stress transport turbulence model employing the symbolic regression approach. *Physics of Fluids, 36*(6), 065108. https://doi.org/10.1063/5.0211608